Cosolvent Effect on the Phase Behavior of Poly(ethylene-*co*-acrylic acid)−Butane Mixtures

Sang-Ho Lee, Minna A. LoStracco, and Mark A. McHugh*

Department of Chemical Engineering, Johns Hopkins University, Baltimore, Maryland 21218

Received July 20, 1995; Revised Manuscript Received October 17, 1995[⊗]

ABSTRACT: Experimental cloud-point data to 250 °C and 2000 bar are presented to demonstrate the impact of dimethyl ether (DME) and ethanol on the phase behavior of poly(ethylene-*co*-acrylic acid) (3.9 mol % acrylic acid) ($EAA_{3.9}$)−butane mixtures. The addition of 6.4 wt % DME to the EAA−butane system decreases the cloud-point pressure from 2000 to 650 bar at 165 °C due to the cross-association of dimethyl ether and acrylic acid in $EAA_{3.9}$. At high DME concentrations, its impact is reduced as the amount of DME increases since polar interactions between excess DME increase after the acrylic acid sites are saturated with DME. Ethanol is a better cosolvent than DME at low ethanol concentrations. The addition of 2.2 wt % ethanol decreases the cloud-point pressure from 2000 to 650 bar at 165 °C due to the cross-association of ethanol and acrylic acid in $EAA_{3.9}$. Ethanol becomes an "antisolvent" at concentrations greater than 16 wt % as excess ethanol self-associates, forming multimers that increase the polarity of the mixture. The cloud-point data are modeled with statistical associating fluid theory (SAFT). The ternary calculations use temperature-independent, binary mixture parameters whose values are obtained by fitting the phase behavior of the three binary pairs that form the ternary system. SAFT correctly predicts the trends observed in the cloud-point curves from zero to 100 wt % DME, although quantitatively it overestimates the effect of DME. SAFT underestimates the effect of ethanol, as the calculated one-phase region is smaller than that observed. However, SAFT correctly predicts the decreasing impact of ethanol with increasing ethanol concentration and that ethanol becomes an antisolvent at high ethanol concentrations.

Introduction

It is well-known that a cosolvent can greatly enhance the solubility of a polymer or copolymer in a number of different ways. If the solvent is less dense than the polymer, the addition of a dense, liquid cosolvent reduces the free volume difference between polymer and solvent and expands the region of miscibility.[1] Also, if the cosolvent specifically interacts with the repeat units of the polymer through complex formation by hydrogen bonding, or if the cosolvent provides favorable physical interactions, such as polar interactions, the region of miscibility expands.[2] Interpreting the effect of a cosolvent on the phase behavior of high-pressure copolymer solutions is slightly more complicated since increasing pressure alone reduces the free volume difference between the solvent mixture and the copolymer and it also modulates the probability of interaction between copolymer, solvent, and cosolvent segments in solution.[3]

There are only a limited number of studies on cosolvency effects with copolymer−solvent mixtures at elevated pressures and, to the best of our knowledge, the copolymers have exclusively been ethylene-based.[3−7] LoStracco, Lee, and McHugh[3] have shown that a nonpolar hydrocarbon cosolvent has virtually no effect on the location of the cloud-point curve for a poly(ethylene-*co*-(31 mol %) methyl acrylate)−propane mixture. Even though the nonpolar cosolvent is very dense, propane is already at liquid-like densities at the kilobar pressures needed to dissolve this copolymer; hence, the cosolvent only incrementally increases solvent density at these high pressures. A result observed for both the poly(ethylene-*co*-methyl acrylate)−solvent[4,5] and poly(ethylene-*co*-vinyl acetate)−solvent[6] systems is that cloud points monotonically decrease in pressure and temperature with the addition of a polar cosolvent that does not form a complex with the polar repeat units in the copolymer. In this case, the cosolvency effect is directly related to the polar forces of attraction contributed by the cosolvent. In contrast, a very large, nonlinear cosolvent effect is observed if the cosolvent forms a complex, or a hydrogen bond, with the polar repeat units in the backbone of the copolymer. In this instance, the cosolvency effect is highly dependent on temperature, concentration of polar repeat units in the backbone of the copolymer, and concentration of cosolvent in solution since complex formation depends on the number of cosolvent and polar repeat units that form complexes. The strength of the interaction of a complex can be up to 1 order of magnitude greater than that of physical interactions associated with dispersion forces.[8,9] As the finite number of repeat units participating in complex formation increases, there is a decrease in the effectiveness of the cosolvent for increasing the region of miscibility. In fact, if the cosolvent can complex with itself, it is possible that the cosolvent will act as an antisolvent causing the copolymer to precipitate from solution once all of the polar repeat units in the copolymer are "titrated" with cosolvent molecules.

The copolymer of interest in this study is poly(ethylene-*co*-(3.9 mol %) acrylic acid) ($EAA_{3.9}$). This copolymer has a melting temperature of 101 °C, a weight average molecular weight of 123 100, and a number average molecular weight of 21 000. Earlier studies have shown that copolymers that contain carboxylic acid repeat units form intra- and interpolymer hydrogen bonds [10−13] and that this characteristic greatly influences the solution properties of acid copolymer−solvent mixtures.[3,14,15] Although the number of acid groups in the backbone of $EAA_{3.9}$ is quite modest, their impact is substantial. Lee et al.[14] show that the cloud-point curves for EAA−butane mixtures shift by ∼26 deg for each mole of acrylic acid added to the backbone of

* To whom correspondence should be addressed.

[⊗] Abstract published in *Advance ACS Abstracts,* January 1, 1996.

0024-9297/96/2229-1349$12.00/0

Table 1. Physical Properties of the Solvents and Cosolvents Used in This Study[16,17]

component	T_c (°C)	P_c (bar)	α ($cm^3 \cdot 10^{25}$)	μ (D)	proton acceptor/donor
n-butane	152.1	38.0	81.4	0.0	
dimethyl ether	126.8	53.0	52.2	1.3	strong acceptor
ethanol	240.8	61.4	51.1	1.7	strong acceptor & donor

the copolymer, a decrease in miscibility that far exceeds the decrease found with increasing molecular weight. Therefore, the polydispersity of the $EAA_{3.9}$ used in this study is not expected to be a primary factor in determining the phase behavior.[3,15]

Table 1 lists the properties of butane and the two cosolvents used in this study, ethanol and dimethyl ether.[16,17] Nonpolar butane, the background solvent used for this study, only interacts by dispersion and induction forces which facilitates the interpretation of the phase behavior when a cosolvent is added to solution. The two cosolvents have identical molecular weights and nearly the same polarizabilities, but the critical temperature of ethanol is much higher than that of dimethyl ether (DME) due to the self-association of ethanol. DME has a dipole moment of 1.4 Debye,[16,17] but more importantly for the work presented here, DME is a proton acceptor (Brønsted base), that can hydrogen bond with proton donors such as carboxylic acids and alcohols.[18] However, DME cannot hydrogen bond to itself since it is not a proton donor. As the concentration of DME in the mixed solvent increases, the polarity of the mixed solvent increases and the number of hydrogen bonds formed between acrylic acid repeat units and DME increases. However, there are only 3.9 mol % acrylic acid repeat units in $EAA_{3.9}$, so once all of the acrylic acid groups are saturated with DME molecules, further addition of DME only contributes to the polarity of the solvent. To correctly interpret the effect of any cosolvent, it is necessary to be cognizant of the binary phase behavior of the solvent−cosolvent mixture. The critical locus of the butane−DME system, which was experimentally measured by de Fernandez et al.,[19] is continuous between the critical points of butane and DME and does not exceed pressures of ~60 bar. Therefore, butane and DME are expected to be completely miscible at the hundreds-to-thousands of bar pressures investigated in this study. Also, DME by itself is an excellent solvent for the ethylene−acid copolymers,[14] so that it is possible to vary the amount of DME in solution from zero to 100%.

The addition of ethanol to butane not only adds polar nature to the mixed solvent, but also creates hydrogen bonds with the acid units in the copolymer. Since ethanol acts as both a proton donor (Brønsted acid) and acceptor (Brønsted base), the phase behavior of $EAA_{3.9}$−butane−ethanol mixtures is influenced by three different types of hydrogen bonds: the cross-association of ethanol molecules and the acrylic acid repeat units of $EAA_{3.9}$, the self-association of the acrylic acid repeat units, and the self-association of ethanol molecules. While acid dimerization and ethanol self-association are unfavorable for producing a single phase, the cross-association of acrylic acid groups and ethanol is favorable to mixing. As the ethanol concentration in the mixed solvent increases, the probability of ethanol self-association becomes greater than the probability of cross-association since there are only 3.9 mol % acid groups in the copolymer which is present at a concentration of ~5 wt % in solution. As a subtle balance

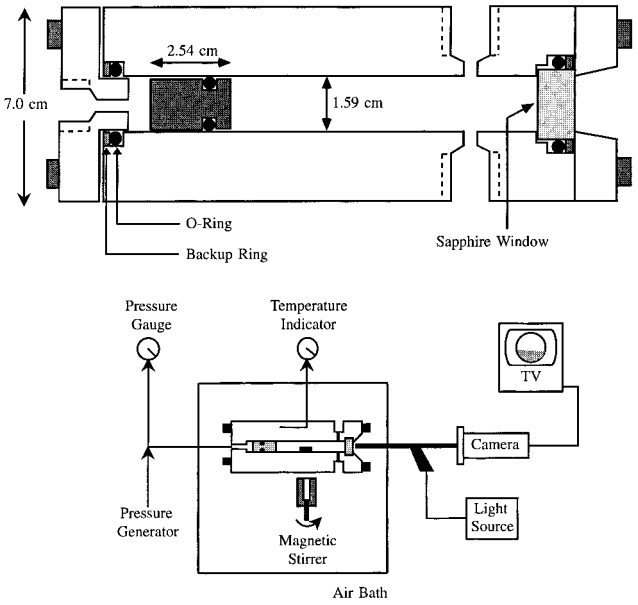

Figure 1. Schematic diagram of the experimental apparatus used in this study to obtain high-pressure cloud-point data.

exists between the cross-association of ethanol with $EAA_{3.9}$, the dimerization of the acrylic acid repeat units, and the self-association of ethanol, interpreting the phase behavior of the $EAA_{3.9}$−butane−ethanol system is expected to be more challenging compared to the behavior of the $EAA_{3.9}$−butane−DME system.

Although there are no literature data available on the phase behavior of butane−ethanol mixtures, the generalized pressure−temperature diagram for this system can be deduced from data for alkane−methanol mixtures. Haarhaus and Schneider[20] show that methanol−butane mixtures do not exhibit any regions of three-phase behavior at temperatures greater than 43 °C. Brunner[21,22] found uninterrupted critical-mixture curves with pressure maximums less than 90 bar, for mixtures of methanol with propane and higher molecular weight alkanes; however, he did not investigate the phase behavior of butane−methanol mixtures. Since ethanol has more hydrocarbon character than methanol, the butane−ethanol system is expected to have a continuous critical-mixture curve with a pressure maximum much less than the hundreds-to-thousands of bar pressures used in the present work.

The experimental cloud-point data obtained in this study are modeled using statistical associating fluid theory (SAFT), which is based on perturbation theory. The equations and strategy used to model the effect of cosolvents on the phase behavior are presented in detail in the modeling section of the paper. The intent of these calculations is to highlight the strengths and limitations of SAFT for calculating the phase behavior of copolymer−solvent−cosolvent mixtures.

Experimental Section

Figure 1 shows the schematic diagram of the experimental apparatus used in this study. Cloud points are obtained with a high-pressure, variable-volume cell that has a 1.59 cm i.d., a 7.0 cm o.d., and a working volume of ~28 cm^3. A 1.9 cm thick sapphire window is fitted in the front part of the cell for observation of the phases. Typically, 0.350 ± 0.002 g of copolymer is loaded into the cell which is subsequently purged several times at room temperature with butane at 3−6 bar to remove any entrapped air. Generally, (5−7) ± 0.020 g of butane is transferred into the cell gravimetrically using a high-pressure bomb which is also used to transfer DME. Ethanol

is transferred into the cell to within ±0.002 g using a syringe. The solution is compressed to the desired pressure with an internal piston that is moved using water displaced by a high-pressure generator. The pressure of the mixture is measured with a Heise gauge (Dresser Ind., model CM−108952, 0−3450 bar, accurate to within ±3.5 bar). Because the measurement is made on the water side of the piston, a small correction (∼1 bar) is added to account for the pressure required to move the piston. The temperature of the cell is measured using a platinum-resistance thermometer (Thermometrics Corp., Class A) connected to a digital multimeter (Keithley Instruments, Inc., Model 195T, accuracy ±0.03%). The system temperature is typically maintained to within ±0.2 deg below 200 °C and to within ±0.4 deg above 200 °C. The mixture inside the cell is viewed on a video monitor using a camera coupled to a borescope (Olympus Corp., model F100-024-000-55) placed against the outside of the sapphire window. Light is transmitted into the cell with a fiber optic cable connected at one end to a high-density illuminator (Dolan−Jenner Industries, Inc., model 180) and at the other end to a borescope. The solution in the cell is well mixed using a magnetic stir bar activated by an external magnet beneath the cell.

Cloud points are obtained at a fixed $EAA_{3.9}$ concentration of ∼5 wt %. The cloud-point pressure is defined as the point at which the mixture becomes so opaque that it is no longer possible to see the stir bar in the solution. The results obtained with this definition of the cloud point have been compared in our laboratories with results obtained using a laser light turbidity measurement where the cloud point is defined as the condition where a 90% decrease in light transmitted through the solution occurs. Cloud points obtained by both methods are identical within the reproducibility of the data. The cloud points are repeated at least twice at each temperature and are typically reproducible to within ±5 bar at the highest temperatures. In the region where the cloud-point pressure increases very rapidly for a small change in temperature, the cloud points are reproducible to within ±10 bar. The lowest temperature of the cloud-point curves presented in this work represents either the highest operating pressure of the experimental apparatus or the location of the copolymer crystallization boundary.

In this study, the solutions are heated and maintained at an elevated temperature (∼250 °C) to reduce the time required to dissolve the copolymer. Normally, experimental data are taken first at a high temperature and then at lower temperatures. After obtaining a cloud-point at the lowest desired operating temperature, the temperature is increased, and one or two high-temperature data points are measured. If there is a discrepancy between data taken at the beginning and the end of an experiment, another independent experiment with fresh solution is performed to determine which data are correct.

Materials

Poly(ethylene-*co*-acrylic acid) was kindly donated by E. I. du Pont de Nemours, Inc. Butane and dimethyl ether, each with a minimum purity of 99%, were obtained from MG Industries and were used as received. Ethanol, with a minimum purity of 99.5% was obtained from Aldrich Chemical Co. and was used as received.

Poly(ethylene-*co*-acrylic acid)−Butane−Dimethyl Ether Phase Behavior

Figure 2 shows the effect of DME on the cloud-point behavior of the $EAA_{3.9}$−butane system. The cloud-point curve for the binary $EAA_{3.9}$−butane system,[14] which is located at higher temperatures and pressures than any of the $EAA_{3.9}$−butane−DME curves, has a large negative slope in pressure−temperature ($P-T$) space. This strong temperature-dependent behavior results from the dimerization of the acrylic acid repeat groups in $EAA_{3.9}$. Even though $EAA_{3.9}$ contains more than 96 mol % nonpolar, ethylene repeat units, nonpolar butane is a poor solvent for this copolymer since the dimerization

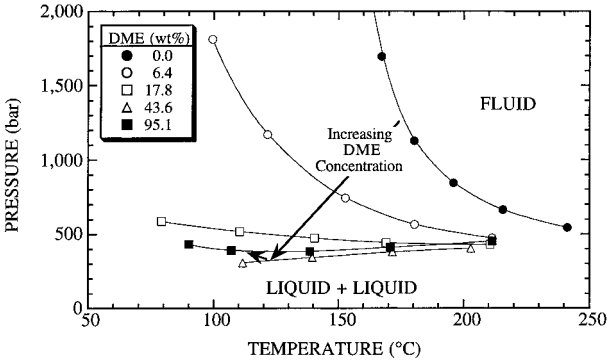

Figure 2. Effect of dimethyl ether (DME) on the phase behavior of the $EAA_{3.9}$−butane system. The $EAA_{3.9}$ concentration is fixed at ∼5 wt % for each solution.

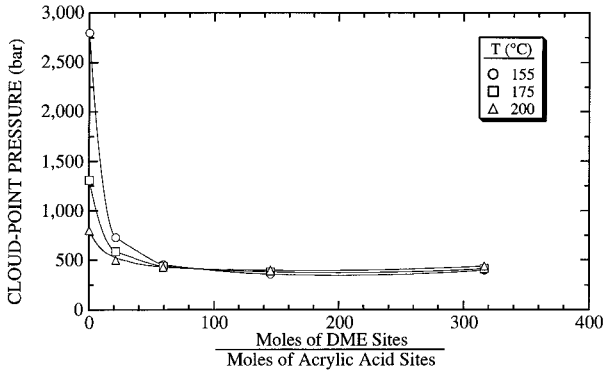

Figure 3. Cosolvent effect of DME on the cloud-point pressures of $EAA_{3.9}$−butane mixtures. The $EAA_{3.9}$ concentration is fixed at ∼5 wt % for each solution.

energy of acrylic acid is much stronger than the dispersion and induction energies between butane and $EAA_{3.9}$.

Adding DME to the $EAA_{3.9}$−butane mixture increases the one-phase region due to the cross-association of acrylic acid with DME. For instance, at 165 °C, the addition of 6.4 wt % DME to an $EAA_{3.9}$−butane mixture drops the cloud-point pressure from 2000 to 650 bar. In contrast, at 165 °C, the cloud-point curve for a ternary mixture containing 43.6 wt % DME is only ∼250 bar lower than the curve for the 6.4 wt % DME mixture. As the concentration of DME in solution exceeds ∼18 wt %, the curves level off or exhibit a slight positive slope in $P-T$ space, indicating that temperature has little influence on cloud-point pressure. Note that the cloud-point curve of $EAA_{3.9}$ in pure DME is located at higher pressures than that of the $EAA_{3.9}$−butane−DME (43.6 wt %) mixture. Also, note that at temperatures over 200 °C, the cloud-point pressures of all the curves appear to converge to ∼500 bar, which is close to the cloud-point pressure of the polyethylene−DME system.[14] At elevated temperatures the solubility behavior of $EAA_{3.9}$ should be similar to that of nonpolar polyethylene because of a significant reduction in the dimerization of acrylic acid groups in $EAA_{3.9}$[12] and in the cross-association of acrylic acid groups with DME. However, the phase behavior is greatly influenced by hydrogen bonding at temperatures below 170 °C.

The impact of DME is presented in a slightly different format in Figure 3. In this figure cloud-point pressure is plotted as a function of DME concentration given in moles of DME sites capable of hydrogen bonding relative to the moles of acrylic acid sites in solution. A single site on one molecule of DME is assumed to interact with a single site on one acid molecule. The impact of DME on the phase behavior is largest for the initial moles of

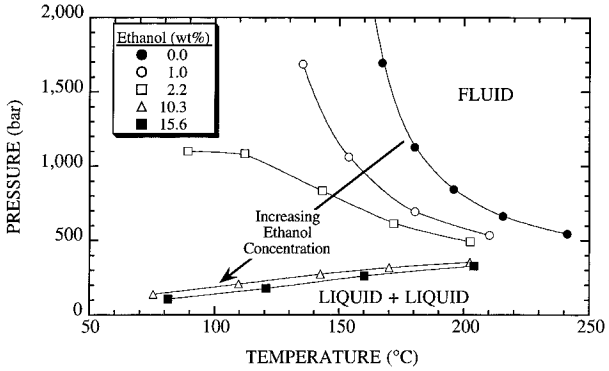

Figure 4. Effect of low concentrations of ethanol on the phase behavior of $EAA_{3.9}$–butane mixtures. The $EAA_{3.9}$ concentration is fixed at ~5 wt % for each solution.

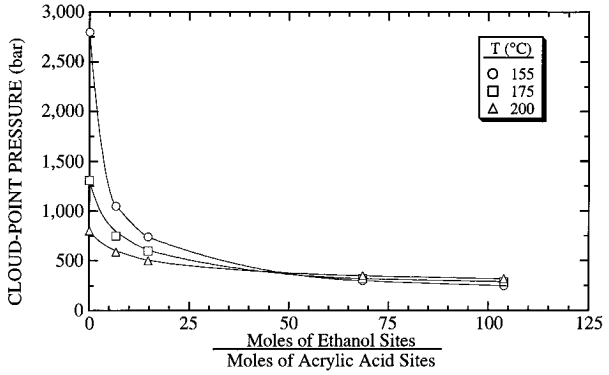

Figure 5. Cosolvent effect of ethanol on the cloud-point pressures of $EAA_{3.9}$–butane mixtures. The $EAA_{3.9}$ concentration is fixed at ~5 wt % for each solution.

DME added to solution at the lowest temperature shown in this figure. Once there are 20 times as many moles of DME sites relative to acid sites there is very little change in the cloud-point pressure for all three temperatures. Using the curves in Figure 3 the maximum effect of DME is estimated to occur at ~100 mol of DME sites/mol of acrylic acid sites, which corresponds to ~30 wt % DME. All three curves in Figure 3 terminate at pure DME solvent which is 325 mol of DME sites/mol of acrylic acid sites since $EAA_{3.9}$ is at 4.9 wt % in solution.

Poly(ethylene-*co*-acrylic acid)–Butane–Ethanol Phase Behavior

Figure 4 shows the effect of small amounts of ethanol on the phase behavior of $EAA_{3.9}$–butane mixtures. Due to cross-association of ethanol and acrylic acid repeat units, the addition of as little as 1.0 wt % ethanol to the $EAA_{3.9}$–butane system decreases the cloud-point pressure by 700 bar at 170 °C. As the ethanol concentration of the mixed solvent increases, the cloud-point curves are located as low as 100 bar and the curves now exhibit positive slopes in $P-T$ space. The effect of ethanol diminishes significantly with increasing ethanol concentration, which is also observed in the phase behavior of $EAA_{3.9}$–butane–DME mixtures. The shape of the cloud-point curves in Figure 4 suggests that at ethanol concentrations greater than 2.2 wt %, the phase behavior is dominated by favorable cross-associations of ethanol and acrylic acid.

The impact of ethanol on the cloud-point pressure is presented in Figure 5. In this figure the moles of ethanol sites capable of hydrogen bonding is equal to twice the number of moles of ethanol in solution since

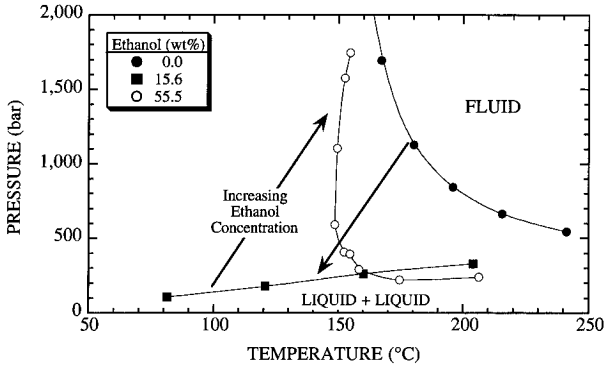

Figure 6. Effect of high concentrations of ethanol on the phase behavior of $EAA_{3.9}$–butane mixtures. The $EAA_{3.9}$ concentration is fixed at ~5 wt % for each solution.

both the hydroxy hydrogen and the oxygen in ethanol can participate in hydrogen bonding with a single acrylic acid molecule. The curves in Figure 5 clearly show that ethanol is initially a more potent cosolvent than DME since the largest drop in cloud-point pressure is obtained with only 5–8 times as many moles of ethanol relative to moles of acid, which is equivalent to 10–16 times as many ethanol sites. Notice also that the three curves in Figure 5 reach a lower minimum, ~250 bar, than do those in Figure 3 for the DME case. The lower minimum pressure of the ethanol systems is probably related to the higher density of ethanol at these temperatures relative to DME, which is above its critical temperature.

Figure 6 shows the effect of high concentrations of ethanol on the phase behavior of $EAA_{3.9}$–butane mixtures. At very high ethanol concentrations many more ethanol molecules are available to self-associate since the bulk of the acrylic acid sites of $EAA_{3.9}$ are expected to be already "titrated" with ethanol molecules. The cloud-point curve at 55.5 wt % ethanol exhibits interesting behavior as a consequence of ethanol–ethanol and ethanol–acrylic acid hydrogen bonding. This curve has a very low minimum pressure with decreasing temperature; it then rapidly rises over a small temperature range and finally shows a slight positive slope with increasing temperature. The shape of this curve suggests that, at high ethanol concentrations, the cloud-point behavior of $EAA_{3.9}$–butane–ethanol mixtures is dominated by the self-association of ethanol as the temperature decreases. On the basis of the results obtained at 55.5 wt % ethanol, it is not surprising that $EAA_{3.9}$ does not dissolve in pure ethanol even to 250 °C and 2000 bar. It is not possible to cross-plot the results in Figure 6 in a manner similar to that in Figures 3 and 5 since the acid copolymer falls out of solution at high ethanol concentrations.

Modeling

Statistical associating fluid theory (SAFT) is used to model the copolymer–solvent–cosolvent phase behavior. The SAFT equation is developed from expressions for the residual Helmholtz free energy, a^{res}, given by

$$a^{res} = (a^{hs} + a^{chain} + a^{assoc}) + a^{disp} \qquad (1)$$

The a^{hs} term, developed by Carnahan and Starling,[23] accounts for segment–segment hard-sphere repulsive interactions; the a^{chain} term, derived on the basis of the associating fluid theory, accounts for the covalent bonds that exist between segments of the molecule,[24] and the a^{assoc} term, also derived by Chapman et al.,[24] is based on the associating fluid theory of Wertheim[25–28] devel-

oped to account for the formation of associations at specific sites on the molecule. The sum of these three terms comprises the reference equation used in SAFT. The a^{disp} term, derived by Alder et al.,[29] represents a perturbation from the reference equation to account for mean-field dispersion and induction interactions. Details on the explicit expressions used for the terms in eq 1 can be found elsewhere and are not reproduced here.[24,30−33]

The residual Helmholtz free energy is used with thermodynamic definitions to derive an equation for the fugacity coefficient, ϕ_i, which is used to calculate phase equilibria.

$$\ln \phi_i = \frac{\mu_i^{res}}{RT} - \ln Z \tag{2}$$

where Z is the compressibility of the mixture, R is the gas constant, T is the temperature, and μ_i^{res} the residual chemical potential which is defined as

$$\frac{\mu_i^{res}}{RT} = \left[\frac{\partial\left(\frac{Na^{res}}{RT}\right)}{\partial N_i}\right]_{T,V,N_{j\neq i}} \tag{3}$$

where N is the total number of moles in the system, N_i represents the number of moles of component i in the system, and V is the total mixture volume. Equation 2 can be rewritten in terms of the residual Helmholtz energy as

$$\ln \phi_i = \left[\frac{\partial\left(\frac{a^{res}}{RT}\right)}{\partial x_i}\right]_{T,V,x_{j\neq i}} - \sum_j x_j \left[\frac{\partial\left(\frac{a^{res}}{RT}\right)}{\partial x_j}\right]_{T,V,x_{k\neq j}} + \frac{a^{res}}{RT} + (Z-1) - \ln Z \tag{4}$$

where x_i is the mole fraction of component i.

The SAFT equation has five pure-component parameters: v^{00}, the temperature-independent volume of a segment; u^0/k, the temperature-independent energy parameter for attraction between two segments; m, the number of segments in a molecule; ϵ^{AB}, the energy of association between sites on a molecule; and v^{AB}, the volume of association. The parameters ϵ^{AB} and v^{AB} are nonzero only for hydrogen-bonding molecules. Mixing rules are required for v^0, the temperature-dependent volume of a segment, for u, the temperature-dependent energy of attraction between two segments, and for m, the average segment size for the mixture. The mixing rule for the volume of a segment is

$$v^0 = \frac{\sum_i \sum_j x_i x_j m_i m_j v_{ij}^0}{\sum_i \sum_j x_i x_j m_i m_j} \tag{5}$$

where

$$v_{ij}^0 = \frac{1}{8}[v_{ii}^{0\,1/3} + v_{jj}^{0\,1/3}]^3 \tag{6}$$

The mixing rule for the energy of attraction between segments is

$$\frac{u}{kT} = \frac{\sum_i \sum_j x_i x_j m_i m_j \left[\frac{u_{ij}}{kT}\right] v_{ij}^0}{\sum_i \sum_j x_i x_j m_i m_j v_{ij}^0} \tag{7}$$

where

$$u_{ij} = (u_{ii}u_{jj})^{1/2}(1 - k_{ij}) \tag{8}$$

and k_{ij} is an adjustable binary mixture parameter. The average segment size for the mixture is

$$m = \sum_i x_i m_i \tag{9}$$

Typically, SAFT is fit to pure component pressure−volume−temperature (PVT) data to determine values for v^{00}, u^0/k, and m. Table 2 shows the pure component parameters of butane, dimethyl ether, and ethanol obtained by Huang and Radosz.[31] Using these parameters, the vapor-pressure curve and saturated liquid densities are reproduced to within ±3% except at conditions very close to the critical point. However, the calculated critical temperatures for these three components are ∼10−17 deg too high and the calculated critical pressures are ∼3−6 bar too high, similar to the results reported by Huang and Radosz[31] for other low molecular weight components. To the best of our knowledge, pure component PVT data do not exist for $EAA_{3.9}$. Since $EAA_{3.9}$ contains ∼96 mol % ethylene repeat units, v^{00} and u^0/k are set equal to the values used for polyethylene. The number of segments of $EAA_{3.9}$ is determined by the correlation developed by Huang and Radosz[31] for polyolefins relating the segment number to the polymer molar mass: $m = 0.05096$ (number average molecular weight).

The energy of acrylic acid association, $\epsilon^{acid-acid}/k$, is determined from spectroscopic measurements of $EAA_{3.9}$.[13,34,35] These investigators found that the enthalpy of hydrogen bond formation for the acrylic acid dimer is equal to ∼11.5 kcal/mol of dimer, which, when divided by the gas constant, gives a value of 5787 K for $\epsilon^{acid-acid}/k$. The dimer forms a cyclic structure with two hydrogen bonds. For the SAFT calculations the one-site model is used for the acid dimerization. It is interesting to note that essentially the same dimerization energy is obtained from spectroscopic data for the acid in the backbone of the copolymer and for monomer acrylic acid.[36] It is difficult to unequivocally determine a value for $v^{acid-acid}$, the site−site volume of association of the dimer in the backbone of the copolymer, since there are only a small amount of data available for these copolymers. In this study $v^{acid-acid}$ is fixed at 0.0339 cm^3/mol, which is similar to the values found by Huang and Radosz[31] when fitting SAFT to pure component data for low molecular weight carboxylic acids. Also, varying the value of $v^{acid-acid}$ by ∼10% has little effect on the calculated results.

As shown in Huang and Radosz,[31] the equations that are used to calculate the contribution of hydrogen bonding involve summations over the different sites. To simplify the calculations, the assumption is made here that the acid sites along the backbone are equivalent regardless of adjacency of the acid groups. Therefore, summations taken over the different sites on an $EAA_{3.9}$ oligomer are replaced by summations over the different *types* of sites multiplied by the number of equivalent

Table 2. Pure Component Parameters for *n*-Butane, Dimethyl Ether, Ethanol, and Poly(ethylene-*co*-acrylic Acid)[a] Used with the SAFT Equation[31]

component	v (cm^3/mol)	m	u/k (K)	ϵ/k (K)	v (cm^3/mol)
n-butane	12.599	3.458	195.11	0	0
dimethyl ether	11.536	2.799	207.83	0[b]	0[b]
ethanol	12.000	2.457	213.48	2758	0.4955
$EAA_{3.9}$	12.000	1070	216.15	5787	0.0339

[a] EAA has 3.9 mol % acrylic acid repeat units in the backbone. [b] Does not self-associate, but is able to form complexes with acrylic acid groups.

Table 3. Association Parameters Used in the SAFT Calculations[a]

	self-association		cross-association	
association parameter	ethanol−ethanol	$EAA_{3.9}$−$EAA_{3.9}$	ethanol−$EAA_{3.9}$	DME−$EAA_{3.9}$
ϵ/k (K)	2758	5787	2825	3356
v (cm^3/mol)	0.4955	0.0339	0.2647	0.0339

[a] The self-association parameters of ethanol are obtained from Huang and Radosz.[31]

sites. An oligomer of $EAA_{3.9}$ has 27 equivalent acid sites and all of them are assumed to participate in hydrogen bonding.

Although it is recognized that molecular weight and molecular weight distribution can have an effect on the location of the cloud-point curve,[37−39] the polydispersity of the copolymer is ignored for the calculations presented here. The first step in the calculation is to determine values of the binary mixture parameters by fitting the phase behavior of the three binary pairs that make up the ternary mixture. The ternary phase behavior is then calculated with no other fitted parameters.

Poly(ethylene-*co*-acrylic acid)−Butane−Dimethyl Ether Calculations. Hasch and McHugh[40] obtain a good fit of the $EAA_{3.9}$−butane cloud-point curve over a temperature range of 170−250 °C with $k_{EAA_{3.9}-butane} = -0.015$. The largest discrepancies between experimental data and calculations occur at high temperatures where there is diminished hydrogen bonding between acid groups in the copolymer. However, these authors point out that their overriding objective is to obtain the best fit of the cloud-point curve in the region of the diagram where the cloud-point pressure increases dramatically with decreasing temperature, thus sacrificing the fit of the cloud-point curve at high temperatures. They also demonstrate that the location of the calculated cloud point is very sensitive to the value of $k_{EAA_{3.9}-butane}$, especially at low temperatures. For the calculations presented here, no attempt is made to determine the effect of $k_{EAA_{3.9}-butane}$ on the ternary phase behavior.

Hasch and McHugh[40] also obtain a good fit of the $EAA_{3.9}$−DME cloud-point curve over a temperature range of 100−250 °C with $k_{EAA_{3.9}-DME} = 0.020$. Table 3 shows the association parameters for the acrylic acid−DME complex used in the SAFT calculations. In these calculations DME is assumed to have one active site similar to that of acrylic acid. It should be noted that SAFT does not explicitly account for polar interactions expected between DME molecules, yet with a reasonably small and temperature-independent value for $k_{EAA_{3.9}-DME}$, a good representation is obtained for the cloud-point curve of the $EAA_{3.9}$−DME binary system. The values of $k_{EAA_{3.9}-DME}$, $\epsilon^{acid-DME}/k$, and $v^{acid-DME}$ reported by

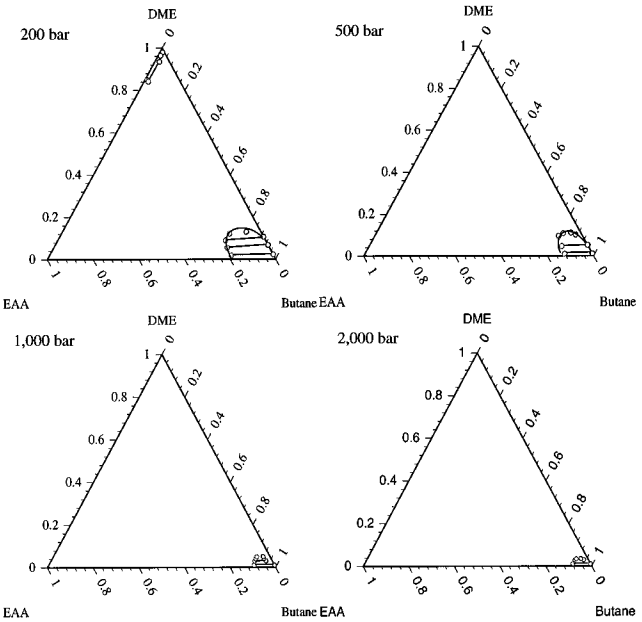

Figure 7. Calculated phase diagrams of the $EAA_{3.9}$−butane−dimethyl ether system at 80 °C and 200, 500, 1000, and 2000 bar. The binary mixture parameter, k_{ij}, is set to −0.015, 0.020, and 0.040 for $EAA_{3.9}$−butane, $EAA_{3.9}$−dimethyl ether, and butane−dimethyl ether, respectively. All concentrations are weight fractions.

Hasch and McHugh[40] are used here without further adjustment.

The value of $k_{butane-DME}$, 0.040, is obtained from a fit of $P-x$ isotherms experimentally measured by de Fernandez et al.[19] It is not possible to obtain a quantitative fit of these isotherms over the entire composition range regardless of the value of $k_{butane-DME}$. However, the calculated critical-mixture pressures are close to the experimental values while the calculated amounts of DME in the vapor and liquid phases are too high.

The cloud-point curves of the ternary system at a fixed $EAA_{3.9}$ composition of ∼5 wt % are obtained by interpolating the calculated results from ternary diagrams at fixed T and P and at various DME concentrations. Only representative ternary diagrams for the $EAA_{3.9}$−butane−DME system at 80 and 160 °C are presented, as diagrams at other temperatures have very similar characteristics. Figure 7 shows four ternary diagrams all at 80 °C and pressures of 200, 500, 1000, and 2000 bar. At 80 °C and 200 bar there are two regions where two phases exist; one at very low DME concentrations and the other at very low butane concentrations. A very large single-phase region exists between these two extreme conditions. Once the pressure is increased to 500 bar, the two-phase region at low butane concentrations disappears. As the pressure is increased further to 2000 bar the other two-phase region at high butane concentrations almost disappears.

The ternary phase diagrams in Figure 8, at 160 °C, exhibit many of the characteristics of those in Figure 7. At 160 °C there is only a single two-phase region at high butane concentrations. This two-phase region shrinks considerably with increasing pressure and it almost disappears at 2000 bar.

Figure 9 shows a comparison of calculated and experimental cloud-point curves for the $EAA_{3.9}$−butane−DME system. The calculated curves at zero, 6.4, 13, and 95.1 wt % DME show that SAFT predicts the maximum cosolvent effect at ∼13 wt % DME as compared to the experimentally observed value of ∼30 wt

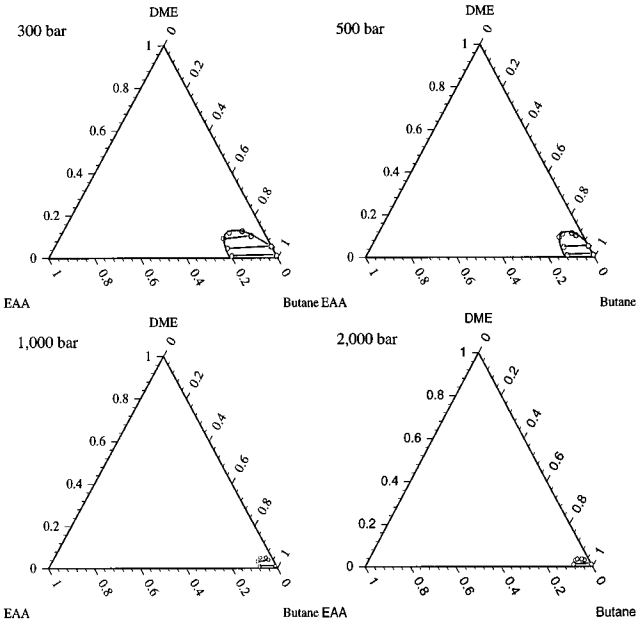

Figure 8. Calculated phase diagrams of the $EAA_{3.9}$−butane−dimethyl ether system at 160 °C and 300, 500, 1000, and 2000 bar. The binary mixture parameter, k_{ij}, is set to −0.015, 0.020, and 0.040 for $EAA_{3.9}$−butane, $EAA_{3.9}$−dimethyl ether, and butane−dimethyl ether, respectively. All concentrations are weight fractions.

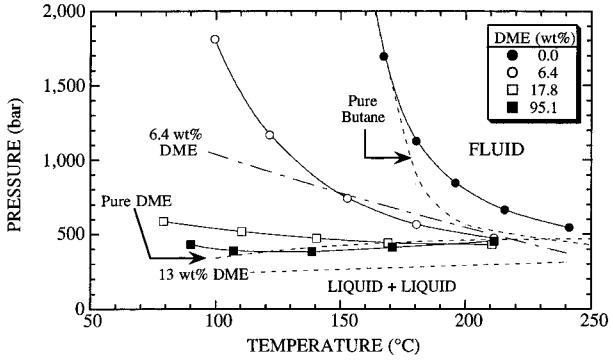

Figure 9. Comparison of experimental and calculated cloud-point curves for $EAA_{3.9}$−butane−dimethyl ether mixtures. The symbols with solid lines represent experimental data obtained in this study, and the dashed lines represent calculations obtained using SAFT. The binary mixture parameter, k_{ij}, is set to −0.015, 0.020, and 0.040 for $EAA_{3.9}$−butane, $EAA_{3.9}$−dimethyl ether, and butane−dimethyl ether, respectively.

%. The calculated curve at 6.4 wt % DME falls below the experimental curve at temperatures less than 150 °C, suggesting that SAFT overpredicts the impact of the cross-association of acrylic acid with DME. Likewise, the calculated curve at 13 wt % is located at ∼250 bar lower than the experimental curve at 17 wt % DME. The calculated curves could be shifted to higher pressures in the low-temperature region of the diagram if $\epsilon^{acid-DME}/k$ were decreased. This was not done here as our objective was to present calculations using as many independently determined parameters as possible. Spectroscopic data are needed to assess the assumption used to obtain a value of the energy of the acid−DME complex. Greater coherence between calculated and experimental curves could also be obtained if the pure component, non-hydrogen bonding parameters for $EAA_{3.9}$ are independently determined as opposed to setting them equal to the parameters used for polyethylene. Pure component *PVT* data are needed to determine the validity of this assumption. Considering the number of assumptions needed to perform these calculations, the fit of the ternary cloud-point curves is quite reasonable and the general trends in the cloud-point behavior as a function of DME concentration are captured by SAFT.

Poly(ethylene-*co*-acrylic acid)−Butane−Ethanol Calculations. For $EAA_{3.9}$−butane−ethanol mixtures, two types of hydrogen bonding occur: self-associations and cross-associations. The energy and volume for the self-association of ethanol are given by Huang and Radosz[31] and are presented in Table 3. Ethanol is assumed to have two associating sites, one on the oxygen and one on the hydroxy hydrogen.[31] As mentioned earlier, the acrylic acid group is assumed to have only one associating site. For the calculations presented here it is assumed that the acrylic acid repeat units are capable of hydrogen bonding with both sites on the ethanol. Since, to the best of our knowledge, there are no acid−alkanol spectroscopic data available in the literature, the value of $\epsilon^{acid-ethanol}/k$, the energy of the acrylic acid−ethanol association, 2825 K, is estimated from the geometric mean of the self-association energies for ethanol and for acrylic acid

$$\epsilon^{acid-ethanol}/k = \left[\frac{1}{2}(\epsilon^{acrylic\ acid}/k)(\epsilon^{ethanol}/k)\right]^{1/2} \quad (10)$$

Note that only half of the acid dimerization energy is used in eq 10 because acid dimerization consists of two bonds, whereas the cross-association between an acid group and an alcohol molecule involves the formation of one bond. The value of $v^{acid-ethanol}$, the association volume of the acrylic acid−ethanol complex, is equal to 0.2647 cm^3/mol, as estimated from the arithmetic mean of the association volumes of acrylic acid dimerization and ethanol self-association

$$v^{acid-ethanol} = \frac{1}{2}[v^{acid-acid} + v^{ethanol-ethanol}] \quad (11)$$

Table 3 lists cross-association parameters of the acrylic acid−ethanol complex used in these SAFT calculations.

For these calculations $k_{EAA_{3.9}-butane}$ remains fixed at −0.015, as previously mentioned. It is not possible to obtain an optimized binary mixture parameter for the $EAA_{3.9}$−ethanol system, since there are no available mixture data for this system in the literature. In screening studies we find that $EAA_{3.9}$ is not soluble in pure ethanol to temperatures of 250 °C and pressures of 2000 bar. Therefore, $k_{EAA_{3.9}-ethanol}$ is set equal to 0.030 to ensure that the calculated, binary $P-x$ isotherms exhibit the so-called "hourglass" shape; that is, they remain open at the top even at extreme operating conditions. The value of the binary mixture parameter for the butane−ethanol system is fit to the $P-x$ isotherm at 72.5 °C, which is the highest temperature isotherm available in the literature.[41] However, the SAFT calculations are in poor agreement with butane−ethanol data regardless of the value of $k_{ethanol-butane}$. Therefore, this mixture parameter is set equal to zero.

Figure 10 shows ternary phase diagrams calculated for the $EAA_{3.9}$−butane−ethanol system at 200 °C and 150, 300, 500, and 1000 bar. All subsequent discussions refer to mixtures containing 5 wt % copolymer since this concentration is used to obtain experimental cloud-point data. At 150 bar, a large two-phase region exists between zero and 100% butane. As the pressure increases, the two-phase region of the diagram breaks into two separate regions. For instance, at 200 °C and 300 bar, two phases are calculated for ethanol concen-

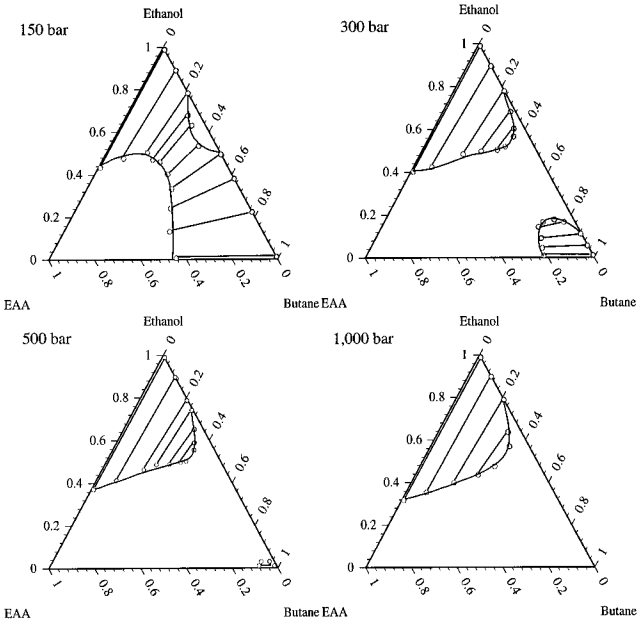

Figure 10. Calculated phase diagrams for the $EAA_{3.9}$–butane–ethanol system at 200 °C and 150, 300, 500, and 1000 bar. The binary mixture parameter, k_{ij}, is set to −0.015, 0.030, and zero for the $EAA_{3.9}$–butane, $EAA_{3.9}$–ethanol, and butane–ethanol systems, respectively. All concentrations are weight fractions.

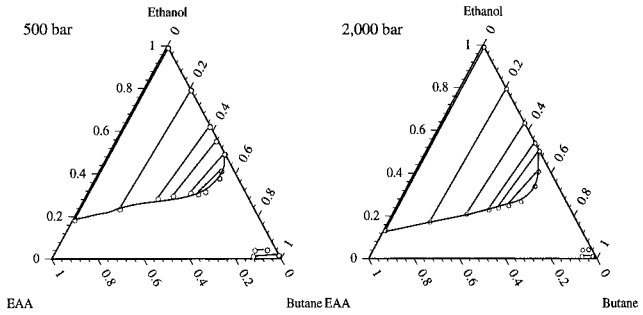

Figure 11. Calculated phase diagrams of the $EAA_{3.9}$–butane–ethanol system at 150 °C and 500 and 2000 bar. The binary mixture parameter, k_{ij}, is set to −0.015, 0.030, and zero for the $EAA_{3.9}$–butane, $EAA_{3.9}$–ethanol, and butane–ethanol systems, respectively. All concentrations are weight fractions.

trations greater than 62 wt % and less than 17 wt %, whereas two phases are experimentally observed for mixtures containing greater than 56 wt % and less than 16 wt % ethanol. The size of the two-phase region at high ethanol concentration increases slightly with increasing pressures and it persists even at pressures of 1000 bar. However, the size of the two-phase region at low ethanol concentrations shrinks considerably as the pressure is increased to 500 bar and it disappears at a pressure between 500 and 1000 bar.

Figure 11 shows ternary phase diagrams calculated using SAFT at 500 and 2000 bar and at 150 °C. At both pressures a large two-phase region exists for butane concentrations less than about 60 wt %. For the mixtures containing a large amount of ethanol cosolvent, increasing the pressure has very little influence on the position of the binodal curve. For mixtures containing large amounts of butane, the two-phase region in Figure 11 at 150 °C and 500 bar is slightly larger than that at 200 °C and 500 bar in Figure 10. At 150 °C, $EAA_{3.9}$–butane–ethanol mixtures with less than ∼5 wt % ethanol remain immiscible even at pressures as high as 2000 bar, while at 200 °C the same

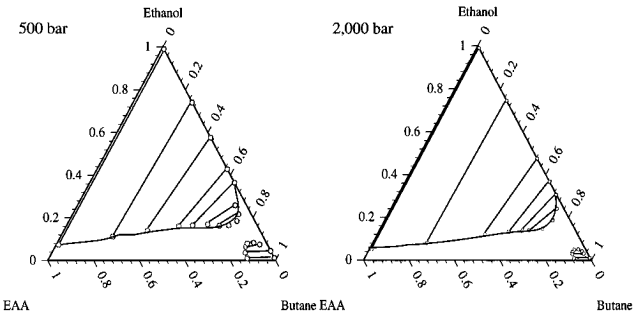

Figure 12. Calculated phase diagrams of the $EAA_{3.9}$–butane–ethanol system at 100 °C and 500 and 2000 bar. The binary mixture parameter, k_{ij}, is set to −0.015, 0.030, and zero for the $EAA_{3.9}$–butane, $EAA_{3.9}$–ethanol, and butane-ethanol systems, respectively. All concentrations are weight fractions.

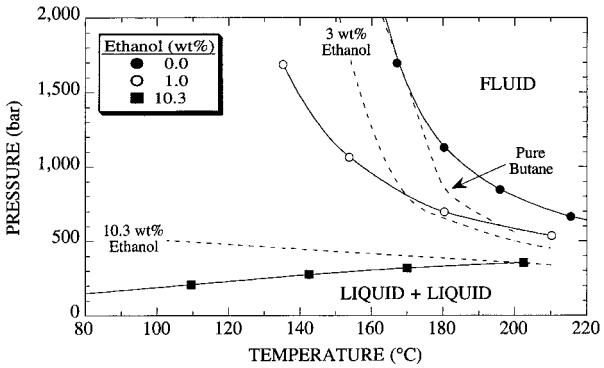

Figure 13. Comparison of experimental and calculated cloud-point curves for $EAA_{3.9}$–butane–ethanol mixtures containing less than 11 wt % ethanol. The symbols with solid lines represent experimental data obtained in this study, and the dashed lines represent calculations obtained using SAFT. The binary mixture parameter, k_{ij}, is −0.015, 0.030, and zero for the $EAA_{3.9}$–butane, $EAA_{3.9}$–ethanol, and butane–ethanol systems, respectively.

mixture becomes totally miscible at pressures slightly greater than 1000 bar.

Figure 12 shows the ternary phase diagrams calculated using SAFT at 100 °C and 1000 and 2000 bar. The characteristics of the behavior in Figure 12 are similar to those at 150 and 200 °C shown in Figures 10 and 11 except that at 100 °C the two-phase region for mixtures with greater than ∼10 wt % ethanol covers a much larger portion of the ternary diagram. Also, at 100 °C and low ethanol concentrations, the size of the two-phase region shrinks at a slower rate with increasing pressure than it did at 150 and 200 °C. This phenomenon means that, at low ethanol concentrations, the calculated cloud-point pressures greatly increase at low temperatures, which is in good qualitative agreement with the experimental observation presented earlier. A two-phase region that extends throughout the entire diagram, similar to that shown in Figure 10 at 150 bar, is found for calculations performed at temperatures below 100 °C regardless of the pressure. At these cold temperatures the acid groups are dimerized and the ethanol molecules are self-associated, leading to a large region of immiscibility.

Figure 13 shows the comparison of experimental and calculated cloud-point curves at low ethanol concentrations. As the ethanol concentration increases from 3 to 10 wt %, the calculated cloud-point curve moves to lower temperatures and pressures, which is in qualitatively good agreement with experimental observations. However, calculated cloud-point pressures are higher than experimental pressures. The difference between

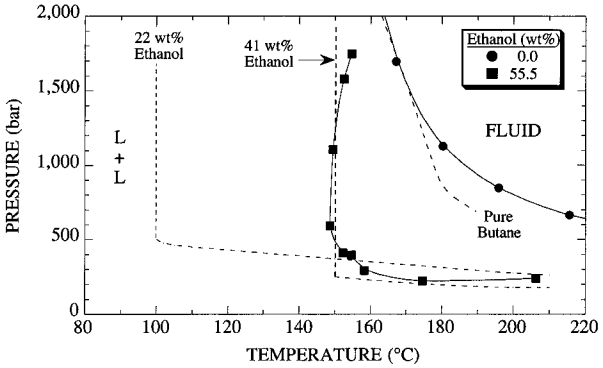

Figure 14. Comparison of experimental and calculated cloud-point curves using SAFT for $EAA_{3.9}$−butane−ethanol mixtures containing greater than 15 wt % ethanol. The symbols with solid lines represent experimental data obtained in this study and the dashed lines represent calculations obtained using SAFT. The binary mixture parameter, k_{ij}, is −0.015, 0.030, and zero for the $EAA_{3.9}$−butane, $EAA_{3.9}$−ethanol, and butane−ethanol systems, respectively.

calculated and experimental cloud-point pressures decreases at high temperatures where hydrogen bonding is diminished except for the $EAA_{3.9}$−butane binary system where the cloud-point pressures are underpredicted at high temperatures as a consequence of forcing the fit of the curve to be closer in the steep region of the diagram. Note also that the calculated curve at 10.3 wt % ethanol exhibits a slight negative slope while the data have a slight positive slope.

Figure 14 shows the comparison of experimental and calculated cloud-point curves at high ethanol concentrations. The calculated curves at 22 and 41 wt % ethanol exhibit the diminishing effect of increased ethanol concentration similar to the trends exhibited by the experimental data. At high temperatures, both of these calculated cloud-point curves are at very low pressures and turn up abruptly, at ∼100 °C for 22 wt % ethanol and at 150 °C for 41 wt % ethanol, indicating that ethanol reverts to antisolvent behavior. The shapes of these two curves are qualitatively similar to the experimental curve at 55.5 wt % ethanol.

In these ternary calculations, the values of $\epsilon^{\text{acid−ethanol}}/k$ and $v^{\text{acid−ethanol}}$ for the acrylic acid−ethanol complex are determined using mixing rules. If the value of $\epsilon^{\text{acid−ethanol}}/k$ is increased, the region of miscibility would increase and the temperature where the cloud-point curve increases dramatically in pressure would be lower for a given concentration of ethanol. Spectroscopic data are needed for acid−ethanol mixtures to independently fix the association parameters.

Conclusions

Previous work has shown that the addition of a small number of acid comonomer groups into the backbone of polyethylene has a dramatic impact on the pressures and temperatures needed to dissolve this type of nonpolar/polar copolymer in a given solvent.[14] In the present work it is shown that adding a polar cosolvent to a nonpolar solvent also has a dramatic impact on the conditions needed to dissolve poly(ethylene-*co*-acrylic acid) copolymers. The two cosolvents investigated, DME and ethanol, both hydrogen bond with the acrylic acid units of $EAA_{3.9}$, which reduces the pressures and temperatures needed to dissolve this copolymer relative to the conditions needed when pure butane is used. Increasing the system temperature attenuates the impact of a polar cosolvent since the strength of polar and hydrogen bonding interactions decreases as these types of interactions are dependent on molecular configurations which are disrupted by thermal energy. Up to about 15 wt %, ethanol has a more dramatic effect on the cloud-point relative to DME. However, the impact of both DME and ethanol diminishes at cosolvent concentrations greater than ∼15 wt % since unfavorable polar interactions between excess cosolvent molecules increase once all the acid sites in $EAA_{3.9}$ are saturated with cosolvent. At low to moderate temperatures ethanol reverts to antisolvent behavior at high concentrations since it readily self-associates, which induces the solution to phase separate.

Statistical associating fluid theory (SAFT) can qualitatively predict the impact of a cosolvent on the phase behavior of poly(ethylene-*co*-acrylic acid)−butane mixtures. Although not explicitly shown here, qualitatively incorrect phase behavior is calculated for the ternary mixtures with DME and ethanol if the three binary mixture parameters are set equal to zero. Therefore, at least a small amount of binary data are needed to obtain a reasonable estimate for the mixture parameters and reasonable estimate of ternary phase behavior. SAFT qualitatively predicts that the calculated cloud-point curve moves to lower temperatures and pressures with increasing DME and ethanol concentration, and it predicts the diminishing effect of these cosolvents at high cosolvent concentrations. It should be possible to obtain a more quantitative representation of the phase behavior of the ternary mixtures if experimental values of the cross-association energies, $\epsilon^{\text{acid−ethanol}}/k$ and $\epsilon^{\text{acid−DME}}/k$, are obtained from spectroscopy. Alternatively, these parameters could be treated as adjustable parameters by following the suggestion of Gregg, Stein, and Radosz.[42]

Acknowledgment. The authors acknowledge the National Science Foundation for support of this project under Grant CTS-9122003.

References and Notes

(1) Cowie, J. M. G.; McEwen, I. J. *Macromolecules* **1974**, *7*, 291.
(2) Wolf, B. A.; Blaum, G. *J. Polym. Sci., Part B: Polym. Phys.* **1975**, *13*, 1115.
(3) LoStracco, M. A.; Lee, S.-H.; McHugh, M. A. *Polymer* **1994**, *35*, 3272.
(4) Hasch, B. M.; Meilchen, M. A.; Lee, S.-H.; McHugh, M. A. *J. Polym. Sci., Polym. Phys. Ed.* **1993**, *31*, 429.
(5) Meilchen, M. A.; Hasch, B. M.; Lee, S.-H.; McHugh, M. A. *Polymer* **1992**, *33*, 1922.
(6) Rätzsch, M. T.; Findeison, R.; Sernow, V. S. *Z. Phys. Chem.* **1980**, *261*, 995.
(7) Wolf, B. A.; Blaum, G. *Makromol. Chem.* **1976**, *177*, 1073.
(8) Huyskens, P. L.; Luck, W. A.; Zeegers-Huyskens, T. *Intermolecular Forces, An Introduction to Modern Methods and Results*; Springer-Verlag: New York, 1991; Chapter 1.
(9) Prausnitz, J. M.; Lichtenthaler, R. N.; de Azevedo, E. G. *Molecular Thermodynamics of Fluid-Phase Equilibria*, 2nd ed.; Prentice-Hall: Englewood Cliffs, NJ, 1986.
(10) Chang, S.-Y.; Morawetz, H. *J. Phys. Chem.* **1956**, *60*, 782.
(11) Longworth, R.; Morawetz, H. *J. Polym. Sci.* **1958**, *29*, 307.
(12) MacKnight, W. J.; Taggart, W. P.; McKenna, L. *J. Polym. Sci.* **1974**, *46*, 83.
(13) Otocka, E. P.; Kwei, T. K. *Macromolecules* **1968**, *1*, 244.
(14) Lee, S.-H.; LoStracco, M. A.; Hasch, B. M.; McHugh, M. A. *J. Phys. Chem.* **1994**, *98*, 4055.
(15) Lee, S.-H.; LoStracco, M. A.; McHugh, M. A. *Macromolecules* **1994**, *27*, 4652.
(16) David, R. L. *CRC Handbook of Chemistry and Physics*, 73rd ed.; CRC Press: Boca Raton, FL, 1992; Chapter 9.
(17) Reid, R. C.; Prausnitz, J. M.; Polling, B. E. *The properties of gases and liquids*, 4th ed.; McGraw-Hill: New York, 1987; Appendix A.

(18) Joesten, M. D.; Schaad, L. J. *Hydrogen Bonding*; Marcel Dekker: New York, 1974.
(19) de Fernandez, M. E.; Calado, J. C. G.; Zollweg, J. A.; Streett, W. B. *Fluid Phase Equilib.* **1992**, *74*, 289.
(20) Haarhaus, U.; Schneider, G. M. *J. Chem. Thermodynam.* **1988**, *20*, 1121.
(21) Brunner, E. *J. Chem. Thermodynam.* **1985**, *17*, 871.
(22) Brunner, E. *J. Chem. Thermodynam.* **1988,** *20*, 273.
(23) Carnahan, N. F.; Starling, K. E. *J. Chem. Phys.* **1969**, *51*, 635.
(24) Chapman, W. G.; Gubbins, K. E.; Jackson, G.; Radosz, M. *Fluid Phase Equilib.* **1989**, *52*, 31.
(25) Wertheim, M. S. *J. Stat. Phys.* **1984**, *35*, 19.
(26) Wertheim, M. S. *J. Stat. Phys.* **1984**, *35*, 35.
(27) Wertheim, M. S. *J. Stat. Phys.* **1986**, *42*, 459.
(28) Wertheim, M. S. *J. Stat. Phys.* **1986**, *42*, 477.
(29) Alder, B. J.; Young, D. A.; Mark, M. A. *J. Chem. Phys.* **1972**, *56*, 3013.
(30) Chapman, W. G.; Gubbins, K. E.; Jackson, G.; Radosz, M. *Ind. Eng. Chem. Res.* **1990**, *29*, 1709.
(31) Huang, S. H.; Radosz, M. *Ind. Eng. Chem. Res.* **1990**, *29*, 2284.
(32) Huang, S. H.; Radosz, M. *Ind. Eng. Chem. Res.* **1991**, *30*, 1994.
(33) Huang, S. H.; Radosz, M. *Ind. Eng. Chem. Res.* **1993**, *32*, 762.
(34) Earnest, T. R., Jr.; MacKnight, W. J. *J. Polym. Sci., Polym. Phys. Ed.* **1978**, *16*, 143.
(35) Kirhara, Y.; Yamamura, H. *J. Polym. Sci., Part B* **1986**, *24*, 867.
(36) Buback, M.; Mahling, F. *J. Supercrit. Fluids* **1995**, *8*, 119.
(37) Koningsveld, R.; Staverman, A. J. *J. Polym. Sci., Polym. Phys. Ed.* **1968**, *6*, 305.
(38) Koningsveld, R.; Staverman, A. J. *J. Polym. Sci., Polym. Phys. Ed.* **1968**, *6*, 325.
(39) Koningsveld, R.; Staverman, A. J. *J. Polym. Sci., Polym. Phys. Ed.* **1968**, *6*, 349.
(40) Hasch, B. M.; McHugh, M. A. *J. Polym. Sci., Polym. Phys. Ed.* **1995**, *33*, 715.
(41) Holderbaum, T.; Utzig, A.; Gmehling, J. *Fluid Phase Equilib.* **1991**, *63*, 219.
(42) Gregg, C. J.; Stein, F. P.; Radosz, M. *Macromolecules* **1994**, *27*, 4972.

MA951043G